

Graph Mixture Density Networks

Federico Errica,¹ Davide Baciucc, ¹ Alessio Micheli ¹

¹Department of Computer Science, University of Pisa

Largo B. Pontecorvo, 3

56127 Pisa, Italy

federico.errica@phd.unipi.it, {baciucc, micheli}@di.unipi.it

Abstract

We introduce the Graph Mixture Density Network, a new family of machine learning models that can fit multimodal output distributions conditioned on arbitrary input graphs. By combining ideas from mixture models and graph representation learning, we address a broad class of challenging regression problems that rely on structured data. Our main contribution is the design and evaluation of our method on large stochastic epidemic simulations conditioned on random graphs. We show that there is a significant improvement in the likelihood of an epidemic outcome when taking into account both multimodality and structure. In addition, we investigate how to *implicitly* retain structural information in node representations by computing the distance between distributions of adjacent nodes, and the technique is tested on two structure reconstruction tasks with very good accuracy. Graph Mixture Density Networks open appealing research opportunities in the study of structure-dependent phenomena that exhibit non-trivial conditional output distributions.

Introduction

Approximating the distribution of a target value y conditioned on the input x is at the core of supervised learning tasks. When trained using common losses such as Mean Square Error for regression or Cross-Entropy for classification, supervised methods are known to approximate the expected conditional distribution of the target given the input, that is, $\langle y|x \rangle$ (Bishop 1994). This is standard practice when we assume that the conditional distribution is unimodal and slight variations in the output are mostly due to random noise.

Still, when the target distribution of a regression problem is not unimodal, most machine learning methods fail to represent it correctly by predicting an averaged value. As a matter of fact, a multimodal target distribution associates more than one possible outcome with a given input sample. To address this problem, the Mixture Density Network (MDN) (Bishop 1994) was proposed to approximate arbitrarily complex conditional target distributions, and it finds application in robotics (Choi et al. 2018), epidemiology (Davis et al. 2020) and finance (Schittenkopf, Dorffner, and Dockner 1998), to name a few. MDNs were designed for input data of vectorial nature, but often real-world problems deal with relational data where the structure has a substantial impact

on the expected outcome. For instance, this is especially true in epidemiology (Opuszko and Ruhland 2013).

For more than twenty years, researchers have put great effort into the adaptive processing of graphs (see recent surveys of Baciucc et al. (2020); Wu et al. (2020)). The goal is to infer the best representation of a structured sample for a given task through different neighbourhood aggregation schemes, graph coarsening and information propagation strategies. It is not difficult to find applications that benefit from the adaptive processing of structured information, such as drug design (Podda, Baciucc, and Micheli 2020), classification in social networks (Yang, Cohen, and Salakhudinov 2016), and natural language processing (Beck, Haffari, and Cohn 2018)

Our main contribution is the proposal of an hybrid approach to handle multimodal target distributions within machine learning methods for graphs, called Graph Mixture Density Network (GMDN). This model outputs a multimodal distribution, conditioned on an input graph, for either the whole structure or its individual entities. As such, it extends the capabilities of the most common deep learning models for graphs. We test GMDN on large epidemiological simulations¹ where both structure and multimodality play an essential role in determining the outcome of an epidemic, and results show that GMDN produces significantly better likelihood scores for this kind of tasks.

As a second contribution, we investigate whether computing the distances between multimodal node distributions can encode the adjacency information of a graph. We show that it is indeed possible to retain such information on two common structure reconstruction task with an excellent degree of accuracy.

Related Works

The problem of training a network to output a conditional multimodal distribution, that is, a distribution with one or more modes, has been studied for 30 years. The Mixture of Experts (MoE) model (Jacobs et al. 1991; Jordan and Jacobs 1994) is one of the first proposals that can achieve the goal, even though it was originally meant for a different purpose. The MoE consists of a multitude of neural networks, also called local experts, each being expected to solve a spe-

¹These will be released upon publication.

cific sub-task. In addition, an MoE uses a gating network to weight the contributions of the local experts for a given input. This way, the model learns to select the experts that are most likely to make the correct prediction. The overall MoE output is then the weighted combination of the local experts' outputs; the reader is referred to Yuksel, Wilson, and Gader (2012) and Masoudnia and Ebrahimpour (2014) for comprehensive surveys on this topic. To output a multimodal distribution, it suffices that each local expert produces the parameters of some chosen unimodal distribution. Finally, notice that the MoE aims at imposing soft competition between the experts, but that may not be necessary when modelling the conditional distribution of the data.

The Mixture Density Network (MDN) of Bishop (1994), instead, reduces the computational burden of training an MoE while allowing the different experts, now called sub-networks, to cooperate. An MDN is similar to an MoE model, but it has subtle differences. First, the input is transformed into a hidden representation that is shared between simpler sub-networks, which increases the overall efficiency. Secondly, this representation is used to produce the gating weights as well as the parameters of the different distributions; hence, the initial transformation should encode all the information needed to solve the task into said representation. As the computational costs of processing the input grow, so does the efficiency of an MDN compared to an MoE. This is even more critical when the input is structured, for example as a sequence (Schittenkopf, Dorffner, and Dockner 1998) or a graph, and requires significant resources to be processed.

In terms of applications, MDNs have been recently applied to epidemic simulation prediction (Davis et al. 2020), where the goal is to predict the multimodal distribution of the total number of infected cases under a compartmental model such as the stochastic Susceptible-Infectious-Recovered (SIR) model (Kermack and McKendrick 1927). In the paper, the authors show that, given samples of SIR simulations with different infectivity and recovery parameters, the MDN could approximate the conditioned output distribution using a mixture of binomials. This result is an important step in the approximation of way more complex compartmental models in a fraction of the time originally required, similarly to what has been done, for example, in material sciences (Pilania et al. 2013). Nonetheless, the work of Davis et al. (2020) makes a strong assumption, that is, the infected network is a complete graph. As stated in (Opuszko and Ruhland 2013), arbitrary social interactions in the network play a fundamental role in the spreading of a disease, and as such predictive models should be able to take them into account.

The automatic and adaptive extraction of relational information from graph-structured data is another long-standing research topic (Sperduti and Starita 1997; Frasconi, Gori, and Sperduti 1998; Micheli 2009; Scarselli et al. 2009), that has recently found widespread application in social sciences, chemistry, and bioinformatics. In a recent past, graph kernels (Ralaivola et al. 2005; Vishwanathan et al. 2010) were the main methodology to process structural information; while still effective and pow-

erful, the drawback of graph kernels is the computational costs required to compute similarity scores between pairs of graphs. Nowadays, the ability to efficiently process graphs of arbitrary topology is made possible by a family of models called Deep Graph Networks² (DGNs). To propagate information across the graph, a DGN stacks graph convolutional layers that iteratively aggregate the neighbouring information of each node. The number of layers reflects the amount of contextual information that propagates (Micheli 2009), very much alike to receptive fields of convolutional neural networks (LeCun, Bengio, and others 1995). There is an increasingly growing literature on the topic which is not covered in this work, so we refer the reader to recent introductory texts and surveys (Bronstein et al. 2017; Battaglia et al. 2018; Bacciu et al. 2020; Wu et al. 2020).

For the above reasons, we propose the Graph Mixture Density Networks to combine the benefits of MDNs and DGNs. This is the first DGN that can learn multimodal output distributions conditioned on arbitrary input graphs.

Graph Mixture Density Networks

A graph is defined as a tuple $g = (\mathcal{V}_g, \mathcal{E}_g, \mathcal{X}_g)$ where \mathcal{V}_g is the set of *nodes* representing entities, \mathcal{E}_g is the set of *edges* that connect pairs of nodes, and \mathcal{X}_g denotes the (optional) node attributes. For the purpose of this work, we do not use edge attributes (while the approach can be straightforwardly extended to consider those if needed), and we assume to deal with the same class of graphs DGNs are usually applied to.

The task under consideration is a supervised regression problem where we aim at learning the conditional distribution $P(y_g|g)$, with y_g being the continuous target label associated with an input graph g in the dataset \mathcal{D} . We assume the target distribution to be multimodal, and as such it cannot be well modelled by current DGNs due to well-known averaging effects between the modes. Therefore, we borrow ideas from the Mixture Density Network (Bishop 1994) and extend the family of deep graph networks with multimodal output capabilities.

From a high-level perspective, we seek a DGN that computes node representations $\mathbf{h}_{\mathcal{V}_g} = \{\mathbf{h}_v \in \mathbb{R}^d, d \in \mathbb{N}, \forall v \in g\}$ as well as a set of “mixing weights” $Q_g \in [0, 1]^C$ that sum to 1, where C is the number of unimodal output distributions we want to mix. Given $\mathbf{h}_{\mathcal{V}_g}$, we then apply C different sub-networks Φ_1, \dots, Φ_C that produce the parameters $\theta_1, \dots, \theta_C$ of C output distributions, respectively. In principle, we can mix distributions coming from different families, but we stick to a single family for simplicity of exposition. Finally, combining the C unimodal output distributions with the mixing weights Q_g produces a multimodal output distribution. We sketch the overall process in Figure 1 for the specific case of epidemic simulations.

More formally, we learn the conditional distribution $P(y_g|g)$ using the Bayesian network of Figure 2. Here, round white (dark) nodes represent unobserved (observed) random variables, smaller squares indicate fixed hyperparameters and larger squares indicate deterministic outputs.

²Bacciu et al. (2020) introduced the term in lieu of GNN to avoid ambiguities and to consider deep non-neural models as well.

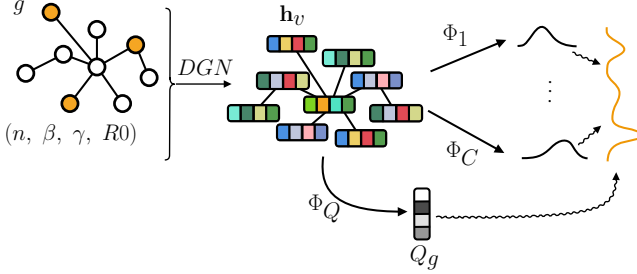


Figure 1: From a high-level perspective, a DGN transforms each node v of the input graph g into a hidden representation \mathbf{h}_v that encodes the structural information surrounding that node. Then, in this work, a subsequent transformation Φ_Q generates the mixing probability vector $Q_g \in [0, 1]^C$ that combines the C different distributions produced by the sub-networks Φ_1, \dots, Φ_C . Similarly to MDNs, the first transformation of the input is shared between the sub-networks. For example, if we were to predict the outcome of a stochastic SIR simulation, orange round nodes might represent initially infected entities in a network of size n , and $\beta, \gamma, R0$ would be simulation-specific node attributes.

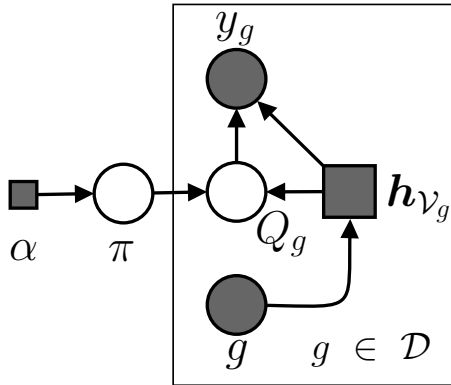


Figure 2: The model can be graphically represented as a Bayesian network where round white (dark) nodes are unobserved (observed) random variables. For each graph g in the dataset \mathcal{D} , we introduce the latent variable Q_g via marginalization. This allows us to break the computation of $P(y_g|g)$ in two steps. The first step encodes the graph information into deterministic node states $\mathbf{h}_{\mathcal{V}_g}$ and produces the posterior distribution $P(Q_g|g)$. In the second and final step, we output the emission distributions $P(y_g|Q_g = i, \mathbf{h}_{\mathcal{V}_g}), i = 1, \dots, C$. The result is a mixture of distributions that depends on the input structure. Finally, the posterior probability is regularized through a Dirichlet prior π whose hyper-parameter α is chosen at model selection time.

The mixing weights Q_g are modelled as a categorical distribution with C possible states. Moreover, we introduce a Dirichlet prior π with hyper-parameter $\alpha = (\alpha_1, \dots, \alpha_C)$ on the distribution $P(Q_g|g)$. The prior is input-independent, and it can prevent the probability mass from collapsing on a single state; this is a well-known problem that has been addressed in the literature through specific constraints (Eigen, Ranzato, and Sutskever 2013) or entropic regularization terms (Pereyra et al. 2017).

In this work, we solve the regression problem by maximum a posteriori (MAP) estimation of the likelihood, where the Dirichlet prior penalizes certain mixing distributions. Given an hypotheses space \mathcal{H} , we seek the MAP hypothesis:

$$h_{MAP} = \arg \max_{h \in \mathcal{H}} P(h|\mathcal{D}) = \arg \max_{h \in \mathcal{H}} P(\mathcal{D}|h)P(h) \quad (1)$$

$$= \arg \max_{h \in \mathcal{H}} \prod_{g \in \mathcal{D}} \sum_{i=1}^C P(y_g|Q_g, \mathbf{h}_{\mathcal{V}_g})P(Q_g|g)\pi(Q_g|\alpha), \quad (2)$$

where we applied the Bayes rule, omitted the constant term $P(\mathcal{D})$ and introduced the latent variable Q_g via marginalization. Notice that $P(h)$ is assumed to be uniformly distributed given the parameters responsible for the categorical distribution $P(Q_g|g)$; in other words, the only parameters that affect $P(h)$ (through the prior distribution π) are those related to $P(Q_g|g)$.

As mentioned earlier, a deep graph network encodes the input graph into node representations $\mathbf{h}_{\mathcal{V}_g}$. Generally speaking, this encoder stacks multiple layers of graph convolutions to generate intermediate node states \mathbf{h}_v^ℓ at each layer $\ell = 1, \dots, L$:

$$\mathbf{h}_v^{\ell+1} = \phi^{\ell+1} \left(\mathbf{h}_v^\ell, \Psi(\{\psi^{\ell+1}(\mathbf{h}_u^\ell) \mid u \in \mathcal{N}_v\}) \right), \quad (3)$$

where ϕ and ψ are (possibly non-linear) functions, and Ψ is a permutation invariant function applied to node v 's neighborhood \mathcal{N}_v . Usually, the final node representation \mathbf{h}_v is given by \mathbf{h}_v^L or, alternatively, by the concatenation of all intermediate states. The convolutions defined in (Kipf and Welling 2017; Xu et al. 2019) are particular instances of Equation 3 that we will use in our experiments.

In graph-prediction tasks, the representations $\mathbf{h}_{\mathcal{V}_g}$ have to be further aggregated using another permutation invariant function Ψ_g

$$\mathbf{h}_g = r_g(\mathbf{h}_{\mathcal{V}_g}) = \Psi_g \left(\{f_r(\mathbf{h}_v) \mid v \in \mathcal{V}_g\} \right), \quad (4)$$

where f_r could be a linear model or a Multi-Layer Perceptron. Equation 4 is often referred to as the “readout” phase. The mixing weights can be computed using a readout r_g^Q as follows:

$$P(Q_g|g) = \sigma(r_g^Q(\mathbf{h}_{\mathcal{V}_g})), \quad (5)$$

where σ is the softmax function over the components of the aggregated vector.

Instead, to learn the emission $P(y_g|Q_g = i, \mathbf{h}_{\mathcal{V}_g}), i = 1, \dots, C$, we have to implement a sub-network Φ_i that outputs the parameters of the chosen distribution. In case the distribution is a multivariate Gaussian, we have

$$\boldsymbol{\mu}_i, \boldsymbol{\Sigma}_i = \Phi_i(\mathbf{h}_g) = f_i(r_g^i(\mathbf{h}_{\mathcal{V}_g})), \quad (6)$$

with f_i being defined as f_r . Note that node-prediction tasks do not need a global readout phase, so Equations 5 and 6 are directly applied to $\mathbf{h}_v \forall v \in \mathcal{V}_g$.

Differently from the Mixture of Experts, which would require a new DGN encoder for each output distribution i , we follow the Mixture Density Network approach and share $\mathbf{h}_{\mathcal{V}_g}$ between the sub-networks. This form of weight sharing reduces the number of parameters and pushes the model to extract all the relevant structural information into $\mathbf{h}_{\mathcal{V}_g}$. Furthermore, using multiple DGN encoders can become computationally intractable for large datasets.

Training. We train the Graph Mixture Density Network using the Expectation-Maximization (EM) framework (Dempster, Laird, and Rubin 1977) for MAP estimation. We choose EM for the local convergence guarantees that it offers with respect to other optimizers. Indeed, by introducing the usual indicator variable $z_i^g \in \mathcal{Z}$, which is one when graph g is in latent state i , we can compute the E-step analytically as in standard mixture models (Jordan and Jacobs 1994; Corduneanu and Bishop 2001):

$$\begin{aligned} \mathbb{E}_{\mathcal{Z}|\mathcal{D}}[\log \mathcal{L}_c(h|\mathcal{D})] &= \\ &= \log \prod_{g \in \mathcal{D}} \prod_{i=1}^C \left\{ P(y_g|Q_g = i, \mathbf{h}_{\mathcal{V}_g}) P(Q_g|g) \right\}^{z_i^g} \end{aligned} \quad (7)$$

where $\log \mathcal{L}_c(h|\mathcal{D})$ is the complete log likelihood of the data. Notice how the prior is not involved in the computation of the E-step. The posterior probability can then be computed as

$$P(z_i^g = 1|g) = \frac{1}{Z} P(y_g|Q_g = i, \mathbf{h}_{\mathcal{V}_g}) P(Q_g|g) \quad (8)$$

where Z is the usual normalization term obtained via straightforward marginalization. On the other hand, we do not have closed-form solutions for the M-step because of the non-linear functions used. Hence, we perform the M-step using gradient ascent to maximize the following term

$$\mathbb{E}_{\mathcal{Z}|\mathcal{D}}[\log \mathcal{L}_c(h|\mathcal{D})] + \sum_{g \in \mathcal{D}} \log \pi(Q_g|\boldsymbol{\alpha}) \quad (9)$$

The resulting algorithm is known as Generalized EM (GEM) (Dempster, Laird, and Rubin 1977); GEM still guarantees convergence to a local minimum if each optimization step improves Equation 9. Our code is publicly available to support reproducibility of all experiments³.

Encoding the structure via distribution distances. In the DGN literature, a common regularization technique encourages adjacent node representations to be similar in the Euclidean space and dissimilar otherwise (Kipf and Welling

³The code to rigorously reproduce all our results will be provided upon publication.

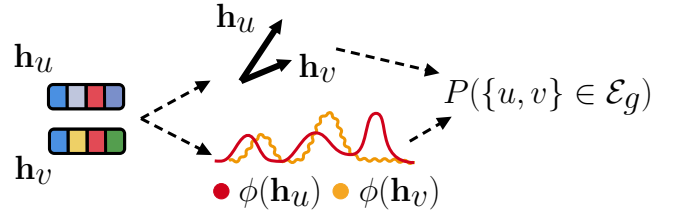


Figure 3: In explicit regularization (top), adjacent node representations must be aligned in the Euclidean space. Instead, we propose to implicitly encode adjacency information (bottom) into the representations $\mathbf{h}_{\mathcal{V}_g}$ by first transforming them into multimodal distributions and then minimizing the distance between adjacent node distributions.

2017). This way, however, the shape of node representations is *explicitly* constrained, and this may limit the amount of information that can be encoded into $\mathbf{h}_{\mathcal{V}_g}$ about the main classification/regression task. For this reason, we propose the first insights into a GMDN-based technique that *implicitly* embeds structural information in the node representations. The idea to use GMDN to produce multimodal distributions for each node with a separate readout module with respect to the main task. Then, we can encourage the distance between pairs of output node distributions, rather than the internal node representations, to be close if the respective nodes are adjacent. For the Data Processing Inequality (Cover 1999), it follows that node representations obtained in this way may encode the structural information without any direct constraint on their shape.

While the application of this strategy to regularization seems promising, one must first investigate whether it is actually possible to learn appropriate distribution distances that encode the adjacency information. This work will take a step in this direction, rather than focusing on regularization benefits, by analyzing the ability of different distance functions to implicitly encode structural information in the node representations. We graphically sketch the idea behind this experiment in Figure 3.

In this context, mixtures of Gaussians prove useful, as there are many possible choices for the distance function. An example is the closed-form L2 distance between two Gaussian mixture distributions P and Q described in Hélen and Virtanen (2007). We define the L2 distance as

$$L_2^2(P, Q) = \int_{\mathbb{R}} (p(x) - q(x))^2 dx. \quad (10)$$

This function sums the point-wise squared distances between the *pdfs* of the two distributions, and it is not difficult to implement in matrix form for univariate Gaussian mixtures (we defer these details to the supplementary material).

Lastly, mapping each node representation into a one-dimensional distribution could also be used as a structure-aware dimensionality reduction technique, in contrast to task-agnostic alternatives commonly used in the literature (Hinton and Roweis 2002; Maaten and Hinton 2008).

Experiments

This section thoroughly describes the datasets, experiments, evaluation process and hyper-parameters used. This work aims at showing that GMDN can fit multimodal distributions conditioned on a graph better than using MDNs or DGNs individually. To do so, we publicly release large datasets of stochastic SIR simulations whose results depend on the underlying network, rather than assuming uniformly distributed connections as in Davis et al. (2020). We generate random graphs using the Barabasi-Albert (BA) (Barabási and Albert 1999) and Erdos-Renyi (ER) (Bollobás and Béla 2001) models. While ER graphs do not preserve the properties of social networks, here we are interested in the emergence of multimodal outcome distributions. We expect GMDN to perform better because it takes both aspects, namely multimodality and structure, into account during training. Then, we analyze whether training on a particular family of graphs exhibits transfer properties; if that is the case, then the model has learned how to make informed predictions about different (let alone completely new) structures. At last, we investigate whether it is possible to encode structural information into $h_{\mathcal{V}_g}$ through the use of distances between distributions, as discussed at the end of the previous section. We compare different distance functions on a structure reconstruction task to show that it is indeed possible to do so.

Datasets. We simulated the stochastic SIR model on Barabasi-Albert graphs of size 100 (BA-100), generating 100 random graphs for different connectivity values (2, 5, 10 and 20). Borrowing ideas from Davis et al. (2020), for each configuration, we run 100 simulations for each different initial infection probability (1%, 5%, 10%) sampling the infectivity parameter β from $[0, 1]$ and the recovery parameter γ from $[0.1, 1]$. The total number of simulations in each dataset is 120.000, and the goal is to predict the distribution of the total infected cases at the end of a simulation. We repeated the process for Erdos-Renyi graphs (ER-100), this time with connectivity parameters 0.01, 0.05, 0.1 and 0.2. Node features consists of β , γ , their ratio $R0 = \beta/\gamma$, a constant value 1, and a binary value that indicates whether that node is infected or not at the beginning of the simulation. The latter is possibly the most important feature, as it lets the model learn how the disease could spread given the network structure. An example of simulation results is summarized in Figure 4.

For the structure reconstruction experiments, we use the Cora and Pubmed datasets (Yang, Cohen, and Salakhudinov 2016), which consist of a single undirected graph of citation documents that are linked together if one cites the other.

Evaluation Setup. We assess the performance of different models using a holdout strategy for the BA and ER datasets (90%/10%/10% split). To make the evaluation more robust, different simulations for the same graph cannot appear in both training and test splits. The metric of interest is the log-likelihood of the data, which captures how well we can fit the target distribution.

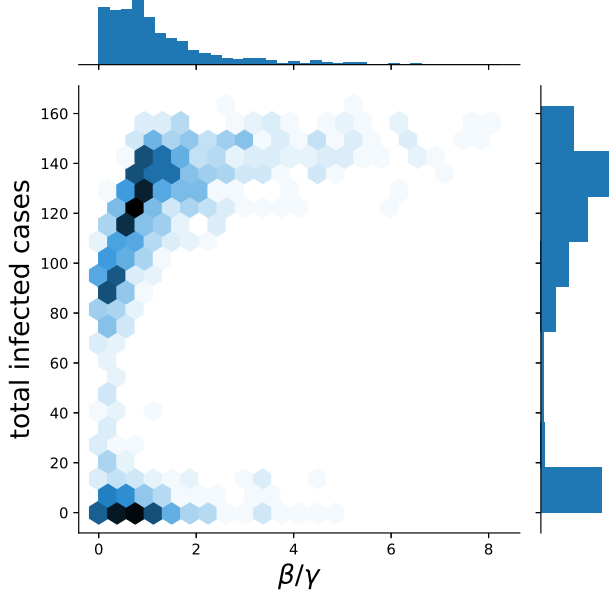


Figure 4: Given a single network and some specific choices for β and γ , the repeated simulation of the stochastic SIR model is known to produce different outcomes. Here we plot the outcome distributions of 1000 SIR simulations on an Erdos-Renyi network of size 200. Depending on the input structure, the distribution of the total infected cases may be multimodal or not, and the GMDN should recognize this phenomenon. In our simulations, larger networks (especially BA ones) exhibited less multimodality; hence, without loss of generality, we focus on larger datasets of smaller graphs.

Instead, we split the links of Cora and Pubmed according to a bootstrap sampling technique. We created ten different 85%/5%/10% link splits with an equal number of true (class 1) and false (class 0) edges. This setup is more robust than using a single split (Kipf and Welling 2017), but it is ten times more expensive because we must perform a model selection for each split. We treat sampled false edges as directed for better exploration of the space of unconnected pairs of nodes. We use an L1 loss with target distance 0 for the positive class and 2 for the negative class. When it comes to computing classification scores, we convert each distance d into a probability using the continuous function $1/(1+d)$ (though hard thresholds are also possible). Following the literature, we evaluate the classification performance using the area under the curve (AUC) and the average precision (AP).

We perform model selection via grid search for all the models presented. We select the best configuration on the validation set using early stopping with patience (Prechelt 1998). After a final re-training, we assess the model’s performance on the unseen test set.

Baselines and hyper-parameters. On BA-100 and ER-100, we compare GMDN against four different baselines. First, RAND predicts the uniform probability $1/n$, where n

is the size of the graph, thus providing the threshold value above which predictions are useful. Instead, HIST computes the normalized frequency histogram of the total infected cases at the end of the simulation. HIST is used to test whether multimodality is useful when a model does not take the structure into account. Finally, we have MDN and DGN, which are, in a sense, ablated versions of GMDN. Indeed, MDN ignores the input structure, whereas DGN cannot model multimodality. Following Davis et al. (2020), neural models are trained to output unimodal (DGN) or multimodal (MDN, GMDN) binomial distributions. The sub-networks Φ_i used are linear models, and the graph convolutional layer is the one from Xu et al. (2019).

For structure reconstruction, we instead consider a GMDN with a multimodal univariate Gaussian output to evaluate different distance functions, all of which exist in closed-form. Apart from the L2 distance we already introduced (GMDN-L2), we tried a variation of the Jeffrey divergence $J(\cdot, \cdot)$ (Jeffreys 1946) that considers weighted mixture components (GMDN-J)

$$J_w(P, Q) = \frac{1}{2} \sum_{i=1}^C w_i^P KL(P_i \parallel Q_i) + w_i^Q KL(Q_i \parallel P_i) \quad (11)$$

where w_i^P and w_i^Q are the mixing coefficients of the i -th component. Similarly, we consider a weighted variant of the Bhattacharyya divergence (GMDN-B). We leave the closed-form derivation of all distances in the supplementary material. All models use the same graph convolutional layer of Kipf and Welling (2017) to remove any source of architectural bias. In what follows, we list the hyper-parameters tried for each model:

- GMDN: $C \in \{3,5\}$, graph convolutional layers $\in \{2,5,7\}$, hidden units per convolution $\in \{64\}$, neighborhood aggregation $\in \{\text{sum}\}$, graph readout $\in \{\text{sum, mean}\}$, $\alpha \in \{1^C, 1.05^C\}$, epochs $\in \{2500\}$, $\Phi_i \in \{\text{Linear model}\}$, Adam Optimizer with learning rate $\in \{0.0001\}$, full batch, patience $\in \{30\}$.
- MDN: $C \in \{2,3,5\}$, hidden units per convolution $\in \{64\}$, neighborhood aggregation $\in \{\text{sum}\}$, graph readout $\in \{\text{sum, mean}\}$, $\alpha \in \{1^C, 1.05^C\}$, epochs $\in \{2500\}$, $\Phi_i \in \{\text{Linear model}\}$, Adam Optimizer with learning rate $\in \{0.0001\}$, full batch, patience $\in \{30\}$.
- DGN: same as GMDN but $C \in \{1\}$ (that is, it outputs a unimodal distribution).
- GMDN-L2/J/B: $C \in \{2,5,10,20,30,50\}$, graph convolutional layers $\in \{1\}$, hidden units per convolution $\in \{128, 256, 512, 1024\}$, neighborhood aggregation $\in \{\text{sum, mean}\}$, $\alpha \in \{1^C\}$, epochs $\in \{2500\}$, $\Phi_i \in \{\text{Linear model}\}$, Adam Optimizer with learning rate $\in \{0.01, 0.001\}$, full batch, patience $\in \{200 \text{ (GMDN-J), } 500\}$.

Results and Discussion

This section discusses our experimental findings. We start from the main empirical study on epidemic simulations, and then we move to the investigation of distribution distances as a way to encode adjacency information.

	BA-100	ER-100	Structure	Multimodal
RAND	-4.60	-4.60	✗	✗
HIST	-1.16	-2.32	✗	✓
MDN	-1.20	-2.45	✗	✓
DGN	-0.75	-2.98	✓	✗
GMDN	-0.67	-1.42	✓	✓

Table 1: Results on BA-100 e ER-100 (12.000 test samples). A higher log-likelihood corresponds to better performances. GMDN improves the performance on both tasks, and this shows that taking into account multimodality and structure together can be helpful.

Epidemic Simulation Results We begin by analyzing the results obtained on BA-100 and ER-100 in Table 1. We notice that GMDN has better test log-likelihoods (12000 test samples) than the other baselines, and the performance gain is particularly significant on ER-100. Being the only model that considers both structure and multimodality, such an improvement in performance was to be expected. However, it is particularly interesting that HIST has a better log-likelihood than MDN on both tasks. By combining this fact with the results of DGN, we come to two conclusions. First, the structural information is the primary factor of performance improvement on BA-100. Secondly, none of the baselines can get close enough to GMDN on ER-100, and therefore this task cannot be solved without looking at structure or multimodality individually. In this sense, BA-100 might be considered an easier task than ER-100, and this is reasonable because multimodality emerges less in the SIR simulations.

Similarly to what has been done in Bishop (1994) and Davis et al. (2020), we analyze how the mixing weights and the distribution parameters vary on a particular GMDN instance. We use $C=5$ and track the behaviour of each sub-network for 100 different ER-100 graphs. Figure 5 shows the value of the mixing weights (left) and of the binomial parameters p (right) for different values of the ratio $R0 = \beta/\gamma$. We immediately see that many of the sub-networks are “shut down” as the ratio grows. Sub-networks 3 and 4 are the ones that control the behaviour of GMDN the most, though for high values of $R0$ only one sub-network suffices. As a matter of fact, when the infectivity rate is much higher than the recovery rate, the target distribution becomes unimodal. The analysis of the binomial parameter for sub-network 4 provides another interesting insight. We observe that, depending on the input graph, the sub-network leads to two possible outcomes, that is, the outbreak of the disease or a partial infection of the network. Note that this is a behaviour that GMDN can model whereas DGN and MDN cannot.

To tell whether GMDN can transfer knowledge to a graph of a different size or belonging to another family, we evaluate the trained models on the datasets shown in Figure 6 while adding the RAND score as the reference baseline. The general trend is that the GMDN trained on ER-100 has better performances than its counterpart trained on BA-100; this is true for all ER datasets, BA-200 and BA-500. This suggests that training on ER-100, known to be “harder”

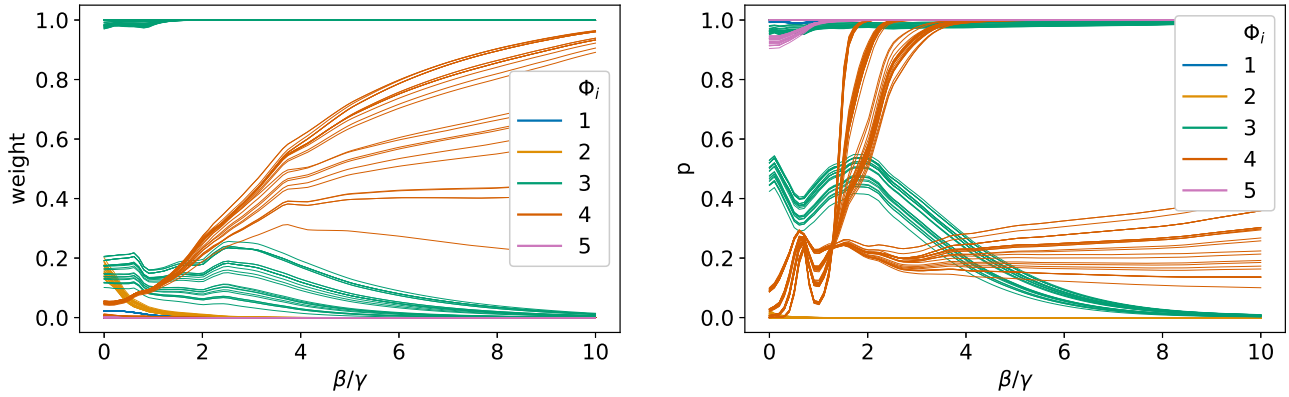


Figure 5: The trend of the mixing weights (left) and binomial coefficient (right) for each one of five sub-networks is shown on 100 ER-100 graphs. We vary the ratio between infection and recovery rate to inspect the behavior of the GMDN. Here, we see that sub-network 4 can greatly change the binomial output distribution in a way that depends on the input graph.

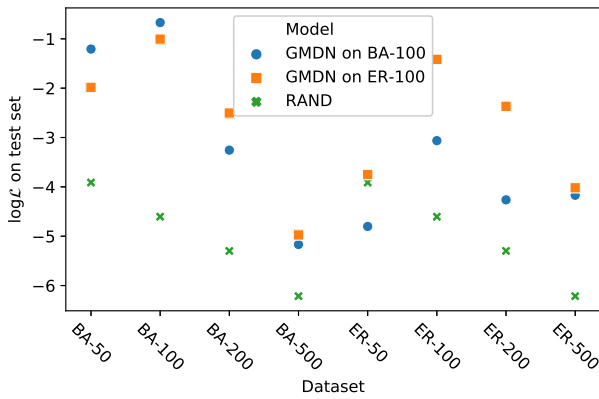


Figure 6: Transfer learning effect of the two trained models, which are shown as blue dots and orange squares. Higher results are better. A GMDN trained on ER-100 exhibits better transfer on larger BA-datasets, which might be explained by the difficulty of the source task.

than BA-100 as discussed above, allows the model to partially learn the dynamics of SIR and transfer them to completely different graphs. Notice that, as the size of the graph changes, the properties of the random graphs also vary, and so obtaining a transfer effect is not that obvious.

Structure Reconstruction via Distribution Distances

Finally, we investigate the ability to implicitly transfer structural information in the node representations by computing the distance between node distributions. We report our structure-reconstruction results in Table 2. In general, all the distance functions perform very well, though the weighted Jeffrey distance is the one with the most satisfactory results. This distance is also more efficient than the L2, which elegantly takes into account Gaussian mixtures but

Model	Cora		Pubmed	
	AUC	AP	AUC	AP
GMDN-B	86.8(1.4)	87.0(1.4)	89.8(1.2)	86.2(1.7)
GMDN-L2	81.6(3.5)	82.9(3.4)	91.8(1.4)	90.2(1.3)
GMDN-J	87.8(1.2)	89.0(1.6)	94.9(0.4)	94.5(0.4)

Table 2: Results for the structure reconstruction tasks. The goal is to show that we can implicitly encode adjacency information inside node representations without forcing adjacent node representations to be aligned in the Euclidean space.

has a quadratic cost in the number of sub-networks. Also, GMDN-L2 was the slowest converging model, possibly due to the complex dependencies between pairs of mixtures.

From these preliminary results, it is clear that distributional distances can be used to reconstruct most of the adjacency information without necessarily imposing explicit constraints on internal node representations. Therefore, future work will further investigate the potential of this technique as a regularization strategy when solving common graph regression/classification tasks.

Conclusions

With the Graph Mixture Density Network, we have introduced a new family of models that combine the benefits of Deep Graph Networks and Mixture Density Networks. These models can solve challenging tasks where the input is a graph and the conditional output distribution is multimodal. In addition, the proper exploitation of node output distributions has provided the first insights into a novel technique that implicitly encodes structural information into node representations. We believe Graph Mixture Density Networks can play an important role in the approximation of structure-dependent phenomena that exhibit non-trivial conditional output distributions.

References

Bacciu, D.; Errica, F.; Micheli, A.; and Podda, M. 2020. A Gentle Introduction to Deep Learning for Graphs. *Neural Networks* 129: 203–221.

Barabási, A.-L.; and Albert, R. 1999. Emergence of scaling in random networks. *Science* 286(5439): 509–512.

Battaglia, P. W.; Hamrick, J. B.; Bapst, V.; Sanchez-Gonzalez, A.; Zambaldi, V.; Malinowski, M.; Tacchetti, A.; Raposo, D.; Santoro, A.; Faulkner, R.; and others. 2018. Relational inductive biases, deep learning, and graph networks. *arXiv preprint arXiv:1806.01261* .

Beck, D.; Haffari, G.; and Cohn, T. 2018. Graph-to-sequence Learning using Gated Graph Neural Networks. In *Proceedings of the 56th Annual Meeting of the Association for Computational Linguistics (ACL), Volume 1 (Long Papers)*, 273–283.

Bishop, C. M. 1994. Mixture density networks .

Bollobás, B.; and Béla, B. 2001. *Random graphs*. 73. Cambridge university press.

Bronstein, M. M.; Bruna, J.; LeCun, Y.; Szlam, A.; and Vandergheynst, P. 2017. Geometric deep learning: going beyond Euclidean data. *IEEE Signal Processing Magazine* 34(4): 25. 18–42.

Choi, S.; Lee, K.; Lim, S.; and Oh, S. 2018. Uncertainty-aware learning from demonstration using mixture density networks with sampling-free variance modeling. In *2018 IEEE International Conference on Robotics and Automation (ICRA)*, 6915–6922. IEEE.

Corduneanu, A.; and Bishop, C. M. 2001. Variational Bayesian model selection for mixture distributions. In *Artificial intelligence and Statistics*, volume 2001, 27–34. Morgan Kaufmann Waltham, MA.

Cover, T. M. 1999. *Elements of information theory*. John Wiley & Sons.

Davis, C. N.; Hollingsworth, T. D.; Caudron, Q.; and Irvine, M. A. 2020. The use of mixture density networks in the emulation of complex epidemiological individual-based models. *PLoS computational biology* 16(3): e1006869.

Dempster, A. P.; Laird, N. M.; and Rubin, D. B. 1977. Maximum likelihood from incomplete data via the EM algorithm. *Journal of the Royal Statistical Society: Series B (Methodological)* 39(1): 1–22.

Eigen, D.; Ranzato, M.; and Sutskever, I. 2013. Learning factored representations in a deep mixture of experts. *International Conference on Learning Representations (ICLR) Workshop* .

Frasconi, P.; Gori, M.; and Sperduti, A. 1998. A general framework for adaptive processing of data structures. *IEEE Transactions on Neural Networks* 9(5): 768–786. Publisher: IEEE.

Helén, M.; and Virtanen, T. 2007. Query by example of audio signals using Euclidean distance between Gaussian mixture models. In *2007 IEEE International Conference on Acoustics, Speech and Signal Processing-ICASSP'07*, volume 1, I–225. IEEE.

Hinton, G. E.; and Roweis, S. T. 2002. Stochastic neighbor embedding. In *Advances in neural information processing systems*, 857–864.

Jacobs, R. A.; Jordan, M. I.; Nowlan, S. J.; and Hinton, G. E. 1991. Adaptive mixtures of local experts. *Neural computation* 3(1): 79–87.

Jeffreys, H. 1946. An invariant form for the prior probability in estimation problems. *Proceedings of the Royal Society of London. Series A. Mathematical and Physical Sciences* 186(1007): 453–461.

Jordan, M. I.; and Jacobs, R. A. 1994. Hierarchical mixtures of experts and the EM algorithm. *Neural computation* 6(2): 181–214.

Kermack, W. O.; and McKendrick, A. G. 1927. A contribution to the mathematical theory of epidemics. *Proceedings of the royal society of london. Series A, Containing papers of a mathematical and physical character* 115(772): 700–721.

Kipf, T. N.; and Welling, M. 2017. Semi-supervised classification with graph convolutional networks. In *Proceedings of the 5th International Conference on Learning Representations (ICLR)*.

LeCun, Y.; Bengio, Y.; and others. 1995. Convolutional networks for images, speech, and time series. *The Handbook of Brain Theory and Neural Networks* 3361(10): 1995.

Maaten, L. v. d.; and Hinton, G. 2008. Visualizing data using t-SNE. *Journal of machine learning research* 9(Nov): 2579–2605.

Masoudnia, S.; and Ebrahimpour, R. 2014. Mixture of experts: a literature survey. *Artificial Intelligence Review* 42(2): 275–293.

Micheli, A. 2009. Neural network for graphs: A contextual constructive approach. *IEEE Transactions on Neural Networks* 20(3): 498–511. Publisher: IEEE.

Opuszko, M.; and Ruhland, J. 2013. Impact of the network structure on the SIR model spreading phenomena in online networks. In *Proceedings of the 8th International Multi-Conference on Computing in the Global Information Technology (ICCGI'13)*.

Pereyra, G.; Tucker, G.; Chorowski, J.; Kaiser, Ł.; and Hinton, G. 2017. Regularizing neural networks by penalizing confident output distributions. *International Conference on Learning Representations (ICLR) Workshop* .

Pilania, G.; Wang, C.; Jiang, X.; Rajasekaran, S.; and Ramprasad, R. 2013. Accelerating materials property predictions using machine learning. *Scientific reports* 3(1): 1–6.

Podda, M.; Bacciu, D.; and Micheli, A. 2020. A Deep Generative Model for Fragment-Based Molecule Generation. In *Proceedings of the 23rd International Conference on Artificial Intelligence and Statistics (AISTATS)*, volume 108, 2240–2250. PMLR.

Prechelt, L. 1998. Early stopping-but when? In *Neural Networks: Tricks of the trade*, 55–69. Springer.

Ralaivola, L.; Swamidass, S. J.; Saigo, H.; and Baldi, P. 2005. Graph kernels for chemical informatics. *Neural Networks* 18(8): 1093–1110. Publisher: Elsevier.

Scarselli, F.; Gori, M.; Tsoi, A. C.; Hagenbuchner, M.; and Monfardini, G. 2009. The graph neural network model. *IEEE Transactions on Neural Networks* 20(1): 61–80. Publisher: IEEE.

Schittenkopf, C.; Dorffner, G.; and Dockner, E. J. 1998. Volatility prediction with mixture density networks. In *International Conference on Artificial Neural Networks (ICANN)*, 929–934. Springer.

Sperduti, A.; and Starita, A. 1997. Supervised neural networks for the classification of structures. *IEEE Transactions on Neural Networks* 8(3): 714–735. Publisher: IEEE.

Vishwanathan, S. V. N.; Schraudolph, N. N.; Kondor, R.; and Borgwardt, K. M. 2010. Graph kernels. *Journal of Machine Learning Research* 11(Apr): 1201–1242.

Wu, Z.; Pan, S.; Chen, F.; Long, G.; Zhang, C.; and Philip, S. Y. 2020. A comprehensive survey on graph neural networks. *IEEE Transactions on Neural Networks and Learning Systems* .

Xu, K.; Hu, W.; Leskovec, J.; and Jegelka, S. 2019. How powerful are graph neural networks? In *Proceedings of the 7th International Conference on Learning Representations (ICLR)*.

Yang, Z.; Cohen, W.; and Salakhudinov, R. 2016. Revisiting semi-supervised learning with graph embeddings. In *International Conference on Machine Learning (ICML)*, 40–48.

Yuksel, S. E.; Wilson, J. N.; and Gader, P. D. 2012. Twenty years of mixture of experts. *IEEE transactions on neural networks and learning systems* 23(8): 1177–1193.